M. Baumann ° & W. Nitsche ▷

Investigation of Active Control of Tollmien-Schlichting Waves on a Wing

Abstract

Experiments were performed to delay the laminar-turbulent transition on a wing by means of active wave cancellation. For this purpose an active wave control system (AWC) was integrated in the instability region of an unswept airfoil (NACA 0012; $c = 800$ mm; $Re_c = 0.8 \cdot 10^6$). Natural 2D flow instabilities were sensed by a surface hot-film-probe, a downstream located actuator (suction/blowing slot) was used to produce a cancelling wave and a further downstream located hot-wire was used to obtain a quality signal of the cancellation process. The sensor-actuator system was operated by a DSP controller (Digital Signal Processor) running an LMS adaptive FIR filter algorithm which performs a feedforward control of the cancellation process. In the experiments, an attenuation of 'natural' broadband TS-waves of 12 dB up to 25 dB was observed at the downstream located error sensor. The highest attenuation rates were obtained when 'natural' instability waves were periodically pre-triggered very lightly by a second suction/blowing slot upstream of the AWC system.

Introduction

Several methods are known to delay the laminar-turbulent transition of boundary layers. These methods can be divided into those which modify the mean velocity profile, such as a negative pressure gradient, suction through the wall or wall cooling in air (wall heating in water) and those which directly influence unstable oscillations dynamically using a wave superposition principle. The linear stability theory of laminar boundary layers suggests the possibility to cancel or to reduce naturally occurring instability waves with artificially excited waves due to linear wave superposition.

In several experimental and numerical investigations the feasibility of active wave cancellation has been verified, but mainly under simplified test conditions such as artificially induced sinusoidal TS-waves instead of randomly occuring natural waves. The basic experimental works of Milling 1981, Liepmann, Nosenchuck & Brown 1982a, 1982b, Thomas 1983 and Gilev & Kozlov 1985, 1987 have clearly shown the feasibility of cancelling artificially induced sinusoidal TS-waves in flat-plate experiments in water and air by means of flush mounted vibrating ribbons, heating strips or periodic suction and blowing through a small slot in the wall. Pilipenko & Shapovalov 1987 were able to reduce 'natural' TS-waves by pure sinusoidal blowing and suction through a slot on a wing. Advanced

attempts to cancel artificially induced broadband TS-waves using feedforward control devices were made by Ladd 1988 on an axisymmetric body with strip-heaters in water, and by Pupator & Saric 1989 on a flat plate employing vibrating ribbons. In both works a very good success in reducing the disturbance levels was reported, e.g. in the work of Pupator & Saric the disturbance level could be reduced by an order of magnitude when compared to the case without control. Later experiments of Ladd 1990 indicated an amplitude reduction of natural TS-waves by approximately 50 % using a simplified feedforward controller compared to his previous work (Ladd 1988) and a suction/blowing-actuator instead of the strip-heater.

Experiments without artificial excitation of instability waves are generally described as conducted under natural conditions, but it is well known that results of such sensitive transition experiments are influenced by disturbances present in the wind- or water tunnel used. Hence, the experiments presented here and which are described in detail in Baumann & Nitsche 1995, can also be classified as conducted under 'natural' conditions. A special case with artificially pre-triggered TS-waves is also presented.

Experimental apparatus

The sensors and the actuator for active TSwave control were located in the instability region of an unswept NACA 0012 wing with a chord of $c = 800$ mm. The experiments were carried out at a velocity of $U_\infty = 14.5$ m/s ($Re_c = 0.8{\cdot}10^6$) in a small closed test section of a wind tunnel at the Institut für Luft- und Raumfahrt of the Technical University Berlin. The freestream turbulence level was approximately 0.2 %. The angle of attack was chosen as $\alpha = 0.36°$ with respect to wall effects in the test section. The adverse pressure gradient obtained $\Delta cp/\Delta x = 0.6$ ($cp_{0.2} = -0.67, cp_{0.5} = -0.49$) corresponds to higher angles of attack under real freestream conditions.

The principle of the active wave control system used on the wing is shown in Fig. 1. The perturbations (TS-waves) are sensed by the first sensor (flush mounted hot-film probe) and from this signal an adaptive controller generates a driver signal for the actuator located downstream ($x/c = 0.43$) to produce an appropriate cancelling wave. The actuator is based on the principle of periodic blowing and suction through a small slot. The actual cancellation effect takes place over a few wave periods downstream. The error sensor (hot-wire probe) delivers a quality or error signal for the optimization or adaptation of the controller in order to achieve a minimum of residual disturbances. The adaptive controller performs a closed loop control due to the continuous adaptation of the unknown transfer function between the perturbation signal and the best possible cancelling signal of the actuator.

The location of the disturbance sensor (surface hot-film probe) was chosen far enough from the actuator to prevent an upstream coupling, which would disturb the adaptation process of the controller (Fig. 1). Additionally small piezofoil-sensors (Nitsche, Mirow & Szodruch 1989) have also been tested as disturbance

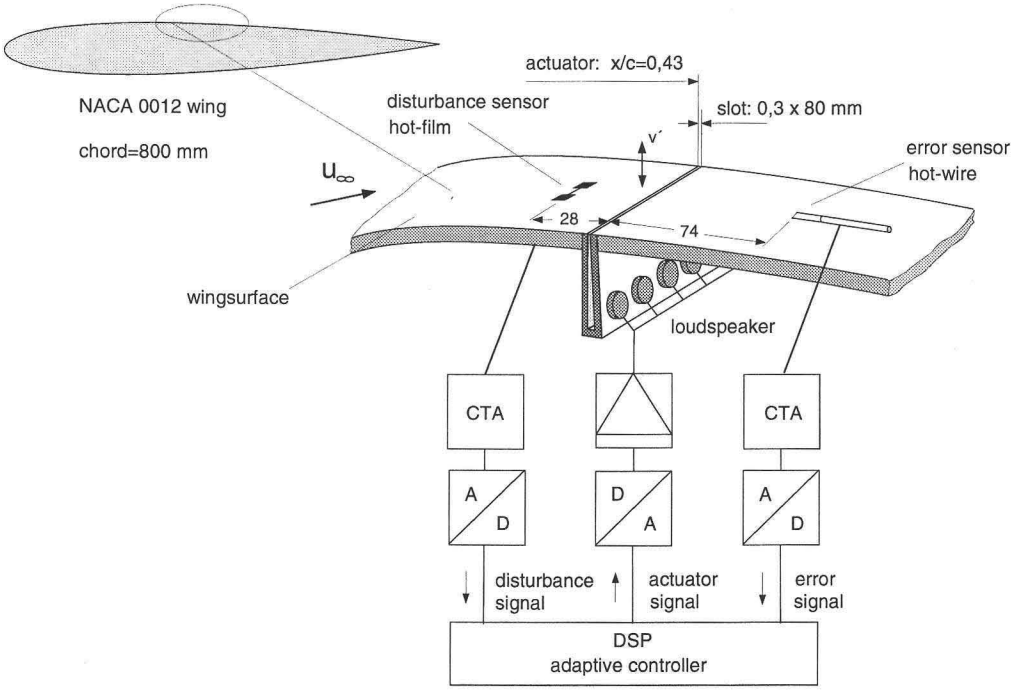

Figure 1: Principle sketch of the developed AWC-System on the NACA test wing.

sensors, but they react more sensitively to upstream coupling due to acoustic effects, which can be observed especially when the adaptation process is not completely finished (Baumann & Nitsche 1995).

The location of the hot-wire error sensor had also to be chosen carefully. It was necessary to keep a certain relaxation distance from the actuator until a homogeneous residual disturbance remains in the boundary layer. Originally, flush mounted hot-film- and piezofoil sensors were too close to the actuator, thus making the wall fixed hot-wire necessary. The wall distance of the hot-wire was chosen approximately to measure the maximum of the u'-fluctuations across the boundary layer. Both sensors were operated in constant-temperature mode (CTA) and their signals were digitalized by A/D-converters of the adaptive control device.

The actuator (Fig. 2) employed consists of a row of small loudspeakers moving the air in a specially shaped cavity which ends as a small slot (0.3 mm wide) in the wing surface and produces a v' velocity component. The chosen geometry combines the advantages of a minimal volume of the wedge shaped cavity and an equalizing effect on differences in the power of any loudspeaker. This results in a good dynamic response of the slot-actuator and in very low deviations in the perturbation velocity v' along the slot. It is known that wedges of 3D-disturbances develop downstream from the lateral ends of the 80 mm long slot, thus only a small area of controlled 2D-disturbances downstream of

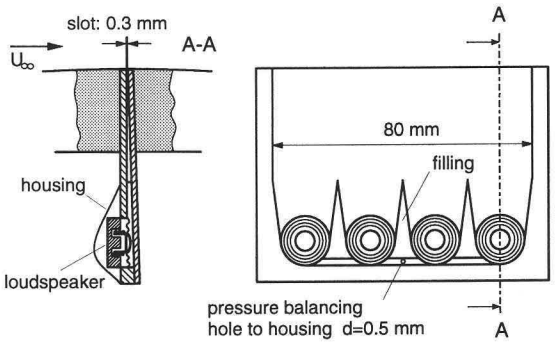

Figure 2: Principle of the suction/blowing-slot actuator.

the mid region of the slot remains. A second actuator (120 mm long) was located upstream ($x/c = 0.25$) of the main sensor-actuator system to enable simplified test conditions with artificial perturbations (excitation with random noise or sinusoidal signals) during the pre-tests of the AWC system.

Adaptive controller

In general, a controller for a sensor-actuator system has two primary functions: to find the time delay between the sensor signal and the actuator signal with respect to the relevant group velocity of the TS-waves and to find the amplification between the signals in order to achieve the best cancellation. Thus, a controller has at least to adapt the delay time and the amplification factor. Ladd 1990 reported an approximately 50 % reduction of 'natural' TS-waves with such a controller. In some preliminary experiments similar values were reached with a very carefully adjusted so-called 'Delay & Amplify' device. In other previous flat-plate experiments we indicated some fluctuations of the group velocity of TS-waves and we further assume that local receptivity effects at the boundary layer actuator and the actuator itself also include nonlinear effects. For these reasons it would be valuable to have a controller which is able to cover most of the still unknown effects with a very fast self adapting transfer function.

Much recent research handles similar problems in active noise control (ANC) applications with modern DSP-based (Digital Signal Processor) electronic devices. The problem of active wave control (AWC) is quite different, but similar tools can be used (Bellanger 1987, Elliott 1993). Especially, the relatively long travel times of TS-waves over the sensor-actuator system require a more complicated controller design. On the other hand the long travel times give enough computing time to model the transfer function more precisely. Fig. 3 shows a block diagram of the implemented feedforward control algorithm, called 'filtered-x-LMS'. The physical transfer function between the disturbance sensor and the actuator (Path 1) is modelled by FIR-filter 1 (Finite Impulse Response). The filter coefficients are derived through an instantaneous adaptation by an LMS-algorithm (Least Mean Square) in order to minimize the signal of the error sensor,

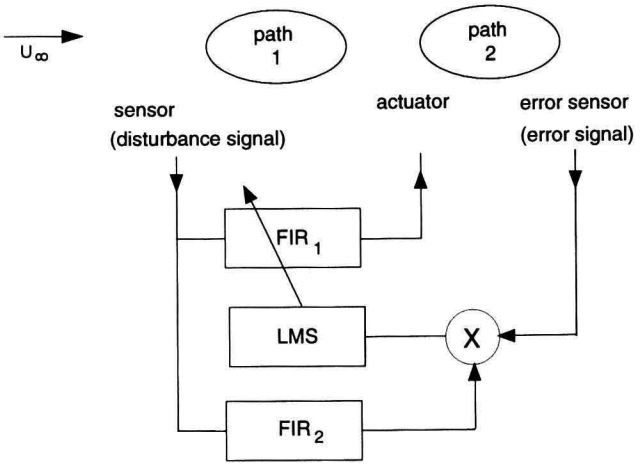

Figure 3: Principle of the adaptive controller (filtered-x-LMS).

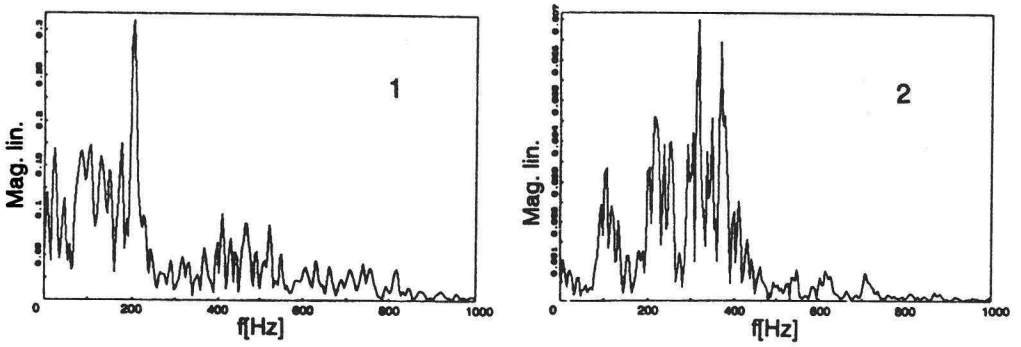

Figure 4: Amplitude spectra of the first and second path FIR filter.

and so minimize the mean square of the error signal. The high time delay between the actuator signal and error signal requires a second FIR-filter 2 to build an internal model of the physical signal path from the actuator to the error sensor (Path 2) ensuring the convergence of the LMS-algorithm. So the disturbance signal is filtered and multiplied by the error signal to generate a filtered reference signal for the LMS-algorithm, which explains the name: 'filtered-x-LMS'. The FIR-filter 2 can be adapted in a pre-training phase by sending random noise to the actuator. In the configuration used each filter vector has 300 coefficients and a sampling rate of 8 kHz was chosen. This means that the whole filter vector of FIR 1 was varied within one sampling period.

The special value of having a fast adapting LMS-algorithm is that the filter coefficients keep moving and thus result in the ability to actually build a more precise transfer function than a well adapted static FIR-filter would be able to do. In consequence the huge amount of fast calculations requires a sophisti-

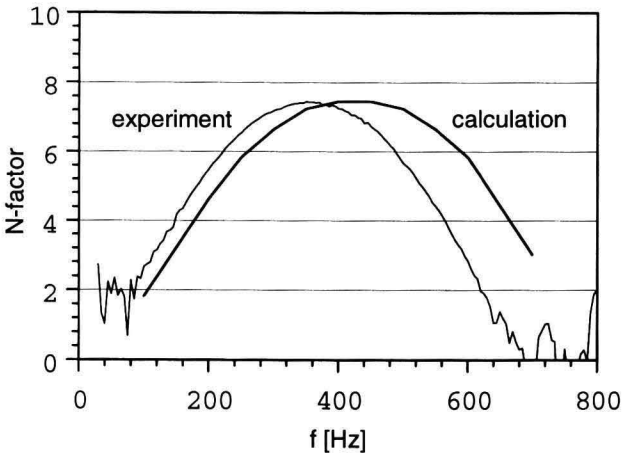

Figure 5: N-factors against frequency at $x/c = 0.5$ (calculation from DASA Bremen).

cated RISC processor like a digital signal processor (DSP). For this reason a fifty megaflop DSP with 16 Bit A/D- and D/A-converters programmed in assembly language was used. The typical convergence time (full adaptation of FIR 1 from zero state) was one minute. Nevertheless the adaptation can follow small fluctuations such as small changes in the angle of attack within increments less than a second, because of the high update frequency. The obtained frequency responses of the adapted filters look very nonuniform. Fig. 4 shows such amplitude spectra of both adapted FIR-filters. They could be of theoretical interest as numerically found transfer functions, but they also include the properties of sensors, the actuator and their amplifiers. Both filters also have a group delay which corresponds to the expected group velocity of the TS-waves.

Stability of the laminar boundary layer

Using the slot-actuators, it was possible to excite very clean sinusoidal TS-waves (excitation by 30 dB of the single frequency above the background perturbations), indicated by the sensors. This made it easy to measure the frequency response between the excitation signal of the first actuator and the hot-film signal in a sine-sweep procedure to indicate the instability frequency range. Fig. 5 shows a comparison between calculated data (performed by DASA Airbus Bremen) and the measured frequency response, scaled as N-factors over the excitation frequency at the hot-film location $x/c = 0.5$. The experiments had to be performed with a reduced angle of attack of $\alpha = 0.36°$ compared to the earlier planned and calculated case with $\alpha = 1.0°$, which could almost entirely explain the difference of the two curves. The second actuator shows a similar behaviour to the first one, except that the boundary layer reacts much more unstably on excitation at the second actuator location. For $\alpha = 1.0°$, the hot-wire already

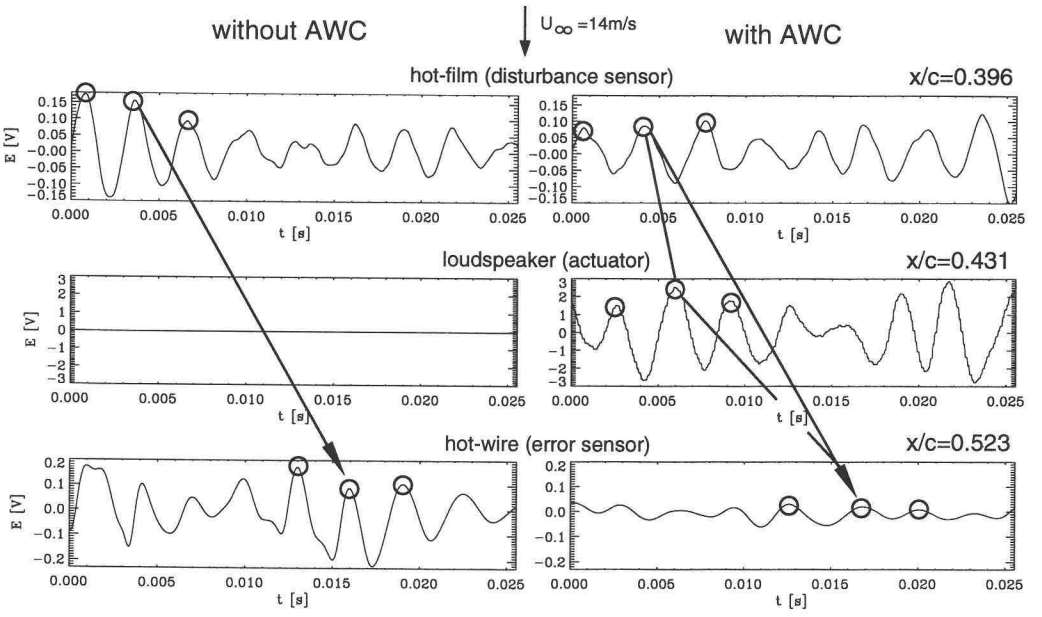

Figure 6: Time traces of the sensor-actuator system without and with control (AWC).

indicates a strong non-linear stage of the 'natural' instability waves, hence the unsuitability of this case for cancellation experiments.

Results of active wave control

During the development phase of the described AWC-system on a wing many simplified pre-tests with artificially excited perturbations were conducted. The results presented, however, will only illustrate the performance of the system under 'natural' flow conditions. Fig. 6 shows two sets of three time traces in downstream order (disturbance sensor, actuator, error sensor). The left set indicates large disturbances at the error sensor, when the actuator is switched off. It can be recognised that some signal peaks correspond to each other and are marked in the figure. The right set shows the three traces when operating the active control device. The signal of the error sensor indicates a significant amplitude reduction of the residual perturbations compared to the case without control. The actuator signal looks similar to that of the disturbance sensor. Characteristic peaks are also marked, indicating different delays from sensor to actuator and actuator to error sensor, which correspond to the different distances.

A comparison of the averaged power spectra of the error sensor signal (with and without AWC) gives a detailed view of the attenuation performance. Fig. 7 shows the power spectra of one of the best obtained damping results. It shows amplitude reductions between 10 dB and 15 dB in the instability frequency range from 200 Hz to 500 Hz. A characteristic value can be found with 12 dB

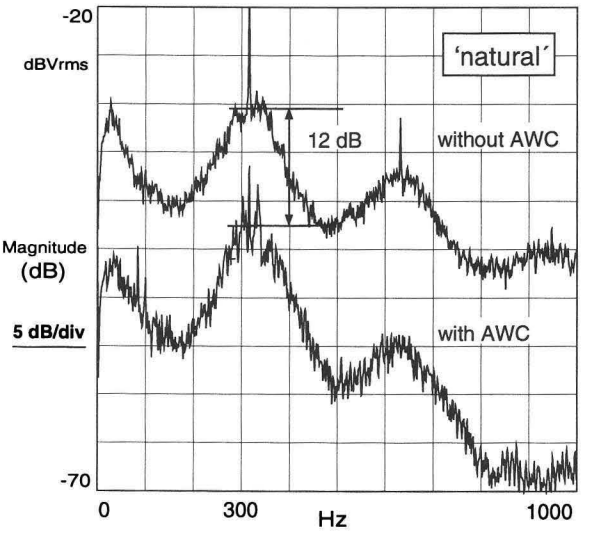

Figure 7: Power spectra of the error sensor with and without AWC, 'natural case'.

at 330 Hz. Much higher differences are reached from 800 Hz to 1000 Hz, which is outside the unstable frequency range and therefore is easier to cancel.

A critical view on the spectra shows why the test conditions have to be classified as quasi natural or even "natural". Especially, the two peaks (at 315 Hz and 630 Hz) in the spectra of Fig. 7 and also of Fig. 8 obviously result from disturbances of the wind tunnel. The AWC-system shows its best performance when reducing peaks in the disturbance spectra, like that at 315 Hz. This depends on the LMS-algorithm and is also known from ANC-applications. As a consequence of this a further experiment was performed with an artificial sinusoidal excitation on the first actuator with a frequency of 344 Hz, which marks the centre of the unstable frequency range. The amplitude was chosen carefully so that the signal of the first sensor indicated almost no change in amplitude but seemed to be more uniform, which looks as though it was triggered periodically. Under these conditions better cancellation effects were observed. The averaged power spectra of Fig. 8 indicate an attenuation between 15 dB and 25 dB. It is to be noticed that an excitation peak at 344 Hz can not be recognized. So it seems to be possible to force a random instability wave with a very small additional artificial excitation to a more uniform 2D-state which is easier to cancel.

Conclusions

Airfoil experiments employing AWC (Active Wave Control) have been successfully conducted. In particular it has been demonstrated that an LMS adaptive FIR-filter (filtered-x-LMS algorithm) in conjunction with a suction/blowing-slot

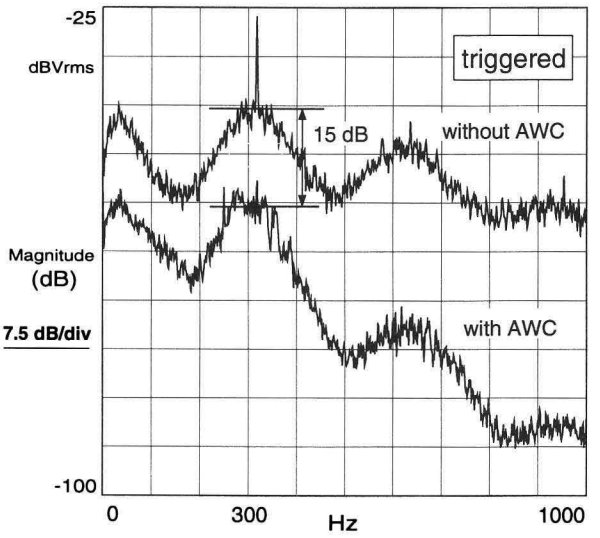

Figure 8: Power spectra of the error sensor with and without AWC, artificially triggered (sine, $f = 344$ Hz).

actuator has the ability to reach very high cancelling effects on 'natural' TS-waves. Amplitude reductions from 12 dB up to 25 dB compared to the case without AWC were observed. This is equivalent to damping factors of 4 up to 18 or expressed as 'negative N-factors' by $N = -1.4$ up to $N = -2.8$. It is of particular interest that the highest attenuation was obtained in case of an artificial triggering of the 'natural' instability waves. This can be explained by the fact that natural instability waves, when artificially 2D-triggered, become less random and probably are forced to a clean 2D-development. In addition, the FIR-filter of the controller can be more precisely adapted to pre-triggered perturbations by the LMS-algorithm and hence cancels TS-waves more effectively.

Questions concerning local effects of the cancellation process and especially concerning the artificial triggering still remain unanswered in this work. But the results obtained give a good basis for further investigations in future work. Especially, active control of artificially pre-triggered 2D-waves (TS-waves) could be a promising research field to understand the local mechanism of such a 'TS-lock-in effect'. It is also of interest to study experimentally whether the method can be used to cancel 3D (primary, secondary) instabilities.

Acknowledgements

The work was partly sponsored by the DASA Airbus (Bremen). Special thanks are to Dr. G. Schrauf, who performed the stability calculations.

References

Baumann, M., Nitsche, W. 1995 – Aktive Grenzschichtbeeinflussung laminar-turbulenter Profilströmungen, ILR-Mitteilung 293 (Jan. 1995), TU-Berlin.

Bellanger, M.G. 1987 – Adaptive Digital Filters and Signal Analysis, New York 1987.

Elliott, S.J., Nelson, P.A. 1993 – Active Noise Control. *IEEE Signal Processing Magazine*, October 1993, 12-35.

Gilev, V.M., Kozlov V.V. 1985 — Use of Small Localized Wall Vibrations for Control of Transition in the Boundary Layer. *Fluid Mechanics-Soviet Research*, **14**, 50-54.

Gilev, V.M., Kozlov V.V. 1987 – Effect of Altering Injection an Suction on Transition in the Boundary Layer. *Fluid Mechanics-Soviet Research*, **16**, 61-68.

Ladd, D.M. 1988 – Active control of 2-D instability waves on an axisymmetric body. *Experiments in Fluids*, **6**, 69-70.

Ladd, D.M. 1990 – Control of Natural Laminar Instability Waves on an Axisymmetric Body. *AIAA Journal*, **28**, 367-369.

Liepmann, H.W., Brown, G.L., Nosenchuck, D.M. 1982a – Control of laminar-Instability waves using a new technique. *J. Fluid Mech.*, **118**, 187-200.

Liepmann, H.W., Nosenchuck, D.M. 1982b – Active control of laminar-turbulent transition. *J. Fluid Mech.*, **118**, 201-204.

Milling, R.W. 1981 – Tollmien-Schlichting wave cancellation. *Phys. Fluids*, **24**, 979-981.

Nitsche, W., Mirow, P., Szodruch, J. 1989 – Piezoelectric Foils as a Means of Sensing Unsteady Surface Forces. *Experiments in Fluids*, **7**, No. 2, 111-118.

Pilipenko, A.A., Shapovalov, G.K. 1987 – Control of Transition to Turbulence in the Boundary Layer by Cancellation of Tollmien-Schlichting Waves by Means of Induced Perturbations. *Fluid Mechanics-Soviet Research*, **16**, 78-85.

Pupator, P.T., Saric, W.S. 1989 – Control of random disturbances in a laminar boundary layer. AIAA Paper 89-1007.

Thomas, A.S.W. 1983 – The control of boundary-layer transition using a wave-superposition principle. *J. Fluid Mech.*, **137**, 233-250.

Authors' address

o Research Scientist
▷ Professor of Aerodynamics
Technische Universität Berlin
Institut für Luft- und Raumfahrt, Sekr. F2
Marchstr. 14, 10587 Berlin, Germany